Amphiphilic Homochiral Oligopeptides Generated *via* Phase Separation of Nonracemic α-Amino Acid Derivatives and Lattice-Controlled Polycondensation in a Phospholipid Environment

by **Irina Rubinstein**[a]), **Gérard Bolbach**[b]), **Markus J. Weygand**[c]), **Kristian Kjaer**[c]), **Isabelle Weissbuch***[a]) and **Meir Lahav***[a])

[a]) Department of Materials and Interfaces, The Weizmann Institute of Science, 76100-Rehovot, Israel (fax: +972-89-34-4138; e-mail: isabelle.weissbuch@weizmann.ac.il; meir.lahav@weizmann.ac.il)

[b]) Laboratoire de Chimie Structurale Organique et Biologique, Université Pierre et Marie Curie, F-75252 Paris Cedex 05

[c]) Materials Research Department, Risø National Laboratory, DK-4000 Roskilde

Dedicated to Professor *Duilio Arigoni* on the occasion of his 75th birthday

Racemic *S*-ethyl thioesters of N^{ε}-stearoyllysine (= *S*-ethyl (*R*,*S*)-2-amino-6-(stearoylamino)hexanethioate) and *S*-ethyl thioesters of γ-stearyl glutamic acid (=stearyl (*R*,*S*)-4-amino-5-(ethylsulfanyl)-5-oxopentanoate) self-assemble as separated two-dimensional crystalline monolayers within an achiral phospholipid environment of racemic 1,2-dipalmitoylglycerol (DPG) and 1,2-dipalmitoylglycero-3-phosphoethanolamine (DPPE), as demonstrated by grazing-incidence X-ray-diffraction (GIXD) measurements performed on the surface of H_2O. Lattice-controlled polycondensation within these crystallites with deuterium-enantiolabeled monomers was initiated by injecting aqueous solutions of Ag^+ or I_2/KI beneath the monolayers, which yielded mixtures of diastereoisomeric oligopeptides containing up to six to eight repeating units, as analyzed by MALDI-TOF mass spectrometry. Analysis of the diastereoisomeric distribution showed an enhanced relative abundance of the oligopeptides with homochiral sequences containing three or more repeating units. Within the DPPE monolayers, the nucleophilic amino group of the phospholipid operates as an initiator of polymerization at the periphery of the monomer two-dimensional crystallites. Enhanced relative abundance of enantiomerically enriched homochiral oligopeptides was obtained by the polycondensation of nonracemic monomers. This enhancement indicated a phase separation into racemic and enantiomorphous monomer crystallites within the phospholipid environment, although this separation could not be observed directly by GIXD. A possible role that might have been played by crystalline assemblies for the abiotic generation and amplification of oligopeptides with homochiral sequences is discussed.

Introduction. – One of the central enigmata in the abiotic origin of life is related to the question of how homochiral biopolymers have been formed under prebiotic conditions. An accepted scenario for early formation of biopolymers from abiotic atomic or molecular ingredients is based on the assumption that primitive polymers might have been formed on surfaces then concentrated and sequestered within primeval membrane-like films that were subsequently converted into proto-cells to form primitive vesicle-like architectures capable of engulfing the polymers for further self-replication [1–3]. This scenario invokes an essential role played by early membrane-like materials in the form of primitive proto-cells. It does not, however, consider the formation of homochiral polymers from racemates or from nonracemic mixtures of activated racemic monomers of low enantiomeric imbalance within these membrane-like environments.

Enantiomerically enriched mixtures of activated amino acids could have been formed in the primitive world either by stochastic kinetic autocatalytic [4][5] or autocrystallization processes [6–9], or by deterministic processes that comprise interactions of nonchiral or racemic materials with circularly polarized light [10], or by nonracemic amino acids from extraterrestrial infall [11].

Polymerization of racemic monomers in ideal solutions generally results in a binomial distribution of polymers of different lengths. Under these circumstances, the formation of longer polymers of homochiral sequence is very improbable. An exception to this trend has been reported recently by *Luisi* and co-workers [12–16] in the polymerization of racemic *N*-carboxyanhydrides of hydrophobic α-amino acids in aqueous solutions.

Recently, we demonstrated an alternative route for the formation of an over-represented amount of isotactic homochiral oligopeptide, starting from amphiphilic activated racemic or nonracemic α-amino acids polymerized within two-dimensional (2D) crystalline domains at the air/water interface [17–19].

Here, we report that a membrane-like environment can be a suitable medium for the synthesis of homochiral oligopeptides from racemic and nonracemic, amphiphilic, activated α-amino acids. This route entails the following events occurring sequentially: *i*) phase separation of the amphiphilic monomers within a phospholipid environment (the phospholipid may segregate either in the form of a crystalline or an amorphous phase); *ii*) self-assembly of nonracemic mixtures of activated α-amino acid monomers such that the minor enantiomer, say (*S*), together with an equal amount of (*R*) forms racemic crystallites, whereas the excess of (*R*) separates into a distinct enantiomorphous phase; and *iii*) catalyst-initiated polycondensation of the monomers within the separated racemic and enantiomorphous crystallites (*Scheme 1*). More specifically, our model environment consists of self-assembled monolayers of 1,2-dipalmitoyl-*rac*-glycerol (*rac*-DPG) or 1,2-dipalmitoyl-*rac*-glycero-3-phosphoethanolamine (*rac*-DPPE) at the air/water interface. We describe here the process of phase separation and polycondensation of the nonracemic *S*-ethyl thioesters of N^{ε}-stearoyllysine (C_{18}-TE-Lys) and γ-stearyl glutamic acid (C_{18}-TE-Glu) occurring within monolayers of *rac*-DPG and *rac*-DPPE at the air/water interface, as studied by grazing-incidence X-ray

Scheme 1

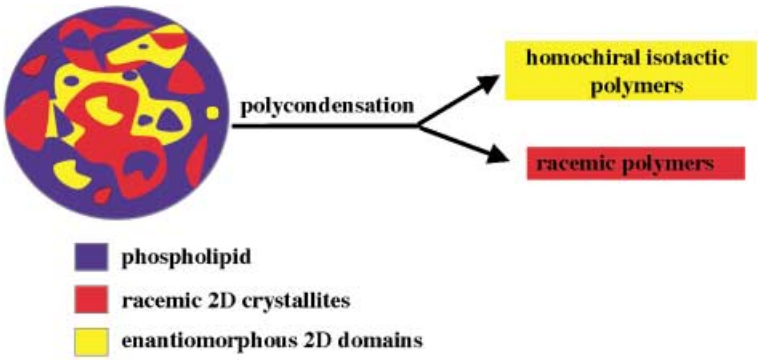

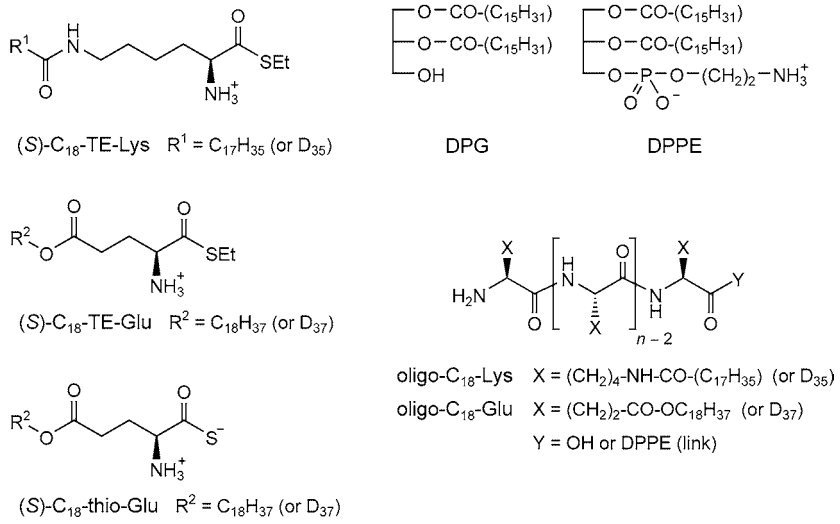

diffraction (GIXD) using synchrotron radiation and by matrix-assisted laser-desorption ionization time-of-flight mass spectrometry (MALDI-TOF MS). Thioesters of α-amino acids are adequate model compounds for the present study since they have been proposed to be plausible precursors of early oligopeptides [20].

Experimental. – *Materials.* The *S*-ethyl thioesters of (*R*)- and (*S*)-N^{ε}-stearoyllysine (= *S*-ethyl (*R*)- and *S*-ethyl (*S*)-2-amino-6-(stearoylamino)hexanethioate; C_{18}-TE-Lys) and the *S*-ethyl thioesters of γ-stearyl (*R*)- and (*S*)-glutamic acid (= stearyl (*R*)- and stearyl (*S*)-4-amino-5-(ethylsulfanyl)-5-oxopentanoate; C_{18}-TE-Glu) were synthesized according to [19]. For the regular series of compounds, we used stearic acid (*Aldrich*) or stearyl alcohol (*Aldrich*), and for deuterated compounds, we used perdeuterated stearic acid (D_{35}, 98%; *Cambridge Isotope Laboratories*) and stearyl alcohol (D_{37}, 98%; *EuroIsotope*). As phospholipids, we used 1,2-dipalmitoyl-*rac*-glycero-3-phosphoethanolamine (*rac*-DPPE) and 1,2-dipalmitoyl-*rac*-glycerol (*rac*-DPG) (*Sigma*). The catalyst I_2/KI was prepared by dissolution of 1.9 g (7.5 mmole) of crystalline I_2 (*Merck*) in an aq. soln. of KI (0.4M, 60 ml). The Ag^+ catalyst was made from $AgNO_3$ (*Aldrich*).

Sample Preparation and Mass-Spectroscopic Characterization. Solns. (0.5 mM) of the mixtures of phospholipid and amphiphilic monomers were prepared in $CHCl_3$ and spread on H_2O, at 20° for a certain nominal molecular area, defined as the area of the trough divided by the total number of molecules spread (see the text). GIXD Measurements were performed after cooling to 4° and purging with He gas at this temp. The polycondensation reactions were initiated by addition of conc. aq. solns. of I_2/KI or $AgNO_3$ as catalysts into the subphase beneath the monolayer to reach a final conc. of 1 and 5 mM, resp. The reaction time was 2–4 h. After the reaction, the monolayer films were compressed with the barrier, and the material, observed by visual inspection, was collected from the liquid surface, transferred to a glass vial, and dried *in vacuo*. Samples for MALDI-TOF MS were then prepared by dissolving the dry material in $CHCl_3$ containing 1% of trifluoroacetic acid. 1 µl of this soln. was deposited on top of a matrix deposit (anthracene-1,8,9-triol soln. in $CHCl_3$/NaI-sat. soln. in THF 1:1) on the instrument holder. MALDI-TOF positive-ion mass spectra were obtained in reflector mode from a *Bruker Biflex 3* instrument equipped with a N_2 laser. External calibration was achieved with calibrating peptides (Substance P, ACTH 8-39) in the mass range studied. Only singly charged ions, *e.g.*, $[M + H]^+$, $[M + Na]^+$, and $[M + 2Na - H]^+$, with the expected isotopic pattern, were observed. Other ions with the same isotopic pattern were often also observed, shifted by $\Delta m/z$ 113 with respect to $[M + Na]^+$ and $[M + 2\,Na - H]^+$, presumably resulting from the formation of an adduct with a trifluoroacetic acid ion (114 Da). In the mass

spectra, the isotopic pattern for a given oligomeric species containing protonated and deuterated units (precision ≥ 0.1 Da) was sufficiently well-defined to correctly assign the monomer composition of the various ions observed. Mass spectra resulted from a signal average of at least several hundreds of laser shots in different spots of the target to get reliable statistical information about the ion peak. Mass assignments were made using both mass-to-charge (m/z) measurement and isotopic-distribution analysis, which is different for protonated and deuterated repeating units. We used the following notation code for the oligopeptides: (h,d) designates a molecule comprising h (S)-deuterated and d (R)-protonated residues, with $n = h + d$ being the total number of repeating units. The rel. abundance of each type of oligopeptide (h,d) is obtained by dividing the intensity of all the ions from a particular molecule by the total intensity of the ions from all the molecules of the same length n. For example, the rel. abundance of a tetrapeptide (4,0) composed of four (R)-protonated chains is calculated as follows: rel. abundance(4,0) = intensity(4,0)/intensity{(4,0) + (3,1) + (2,2) + (1,3) + (0,4)}. The rel. abundance of the tetrapeptide (2,2) composed of two (R)-protonated and two (S)-deuterated chains is calculated as rel. abundance(2,2) = intensity(2,2)/intensity{(4,0) + (3,1) + (2,2) + (1,3) + (0,4)}. A very similar ionization yield is expected for the (h,d) oligopeptides of the same length $n = h + d$ (identical chemical properties). In addition, the very close masses of these compounds and the very close ion velocities made it reasonable to assume similar detection efficiencies. Thus, the ion intensity of the different (h,d) oligopeptides were directly and reliably comparable. Enhancement factors were calculated by dividing the rel. abundance of any oligopeptide by the corresponding experimental values calculated for a theoretical random process.

GIXD Measurements. Experiments were performed with the liquid-surface diffractometer mounted at the *BW1* synchrotron beamline at *Hasylab*, DESY, Hamburg. Details about the exper. technique and the instrument are reported in [21]. The recorded GIXD patterns are represented as two-dimensional contour maps of the scattered intensity, $I(q_{xy}, q_z)$, as a function of the horizontal q_{xy} and vertical q_z components of the scattering vector. The unit-cell dimensions of the 2D lattice were derived from the q_{xy} positions of the *Bragg* peaks. The full-width at half maximum of the *Bragg* peaks (corrected for instrument resolution), FWHM(q_{xy}), gives an estimate of the crystalline coherence length $CL_{hk} \approx 0.9(2\pi/\text{FWHM}(q_{xy}))$ associated with each h,k reflection.

Results and Discussion. – Mixtures of each of the racemic or nonracemic C_{18}-TE-Lys and C_{18}-TE-Glu monomers with either *rac*-DPPE or *rac*-DPG were spread on a H_2O surface at 20° for a nominal molecular area of 40 and 45 Å^2, respectively. GIXD Measurements were performed after cooling the H_2O subphase to 4°. The experiments were performed with monomers with perdeuterated stearyl chains that yielded a difference between the enantiomers [12][21] of 35 and 37 mass units, respectively. The polycondensation reactions, performed at 20 or 4°, were initiated by injection of aqueous solutions containing $AgNO_3$ [23] or I_2/KI [24]. The reaction time was set to 2 h. The oligopeptides were collected from the H_2O surface, and their diastereoisomeric distribution was determined by MALDI-TOF-MS. No measurable isotope effects were observed on interchanging the deuterium labeling of the two enantiomers or the enantiomeric excess in the nonracemic mixtures of monomers.

S-*Ethyl Thioester of* N$^{\varepsilon}$-*Stearoyllysine.* a) *DPG Environment.* The GIXD patterns of equimolar mixtures of *rac*-DPG with (R,S)-C_{18}-TE-Lys (*Fig. 1*,*a*) show a phase separation. One phase corresponds to the diffraction pattern of the self-assembled *rac*-C_{18}-TE-Lys crystallites and is very similar to that measured in the absence of DPG (*Fig. 1*,*c*) [17][19]. The second phase arises from the DPG crystallites, and only one *Bragg* peak is visible, when compared to the GIXD pattern measured for the pure phospholipid (*Fig. 1*,*d*). The surface occupancy of the *rac*-C_{18}-TE-Lys crystallites was only one third of the monolayer total surface and, thus, their crystalline coherent lengths (*CL*s), determined from FWHM(q_{xy}) of the *Bragg* peaks, were somewhat affected by the presence of DPG from 650 and 360 to 450 and 310 Å along the {1,1} and {1, – 1} directions, respectively. The *CL* of the *rac*-DPG crystallites was 180 Å.

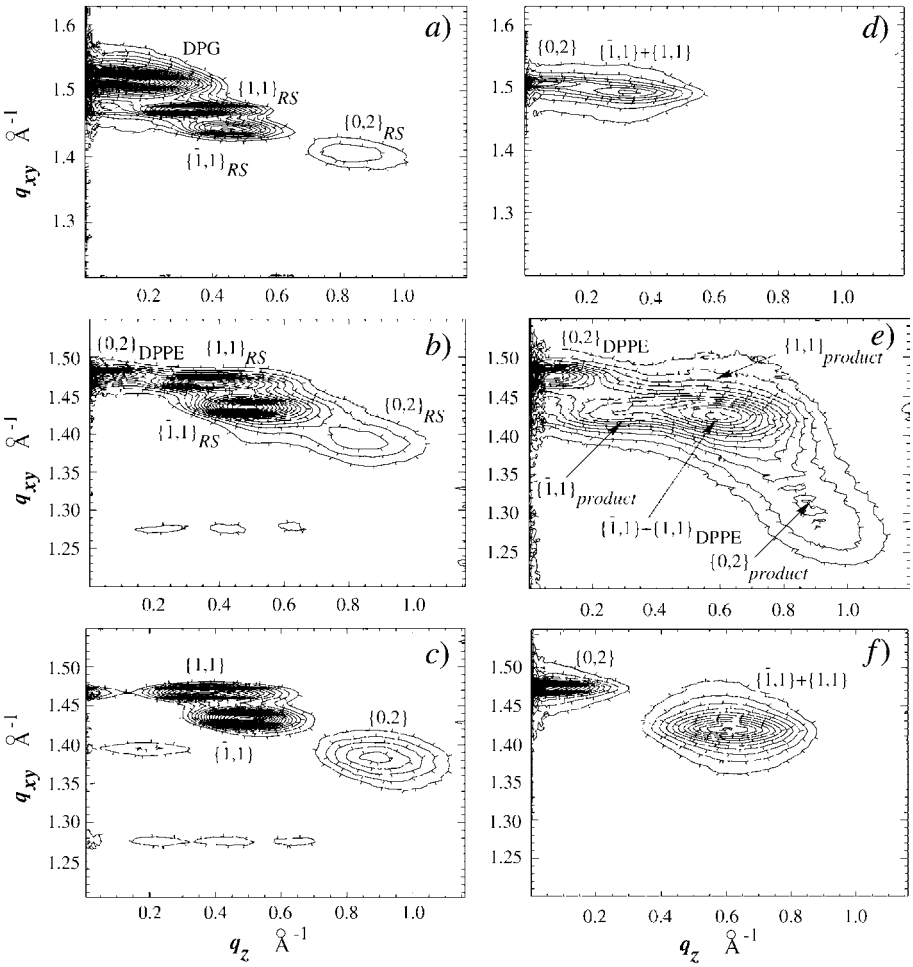

Fig. 1. *GIXD Patterns* (represented as 2D contour maps of scattered intensity I as a function of the horizontal (q_{xy}) and vertical (q_z) components of the scattering vector, measured on H_2O at 4°) *of crystallites self-assembled by spreading $CHCl_3$ solutions of* a,b) *equimolar mixtures of* rac-*C_{18}-TE-Lys with* rac-*DPG and* rac-*DPPE resp.;* c) rac-*C_{18}-TE-Lys*; d) rac-*DPG;* e) *equimolar mixture of* rac-*C_{18}-TE-Lys with* rac-*DPPE after 2 h in the presence of Ag^+*; f) rac-*DPPE*. The *Bragg* peaks are labeled by their {*h*,*k*} *Miller* indices and the subscripts '*R*,*S*' refer to the (*R*,*S*)-C_{18}-TE-Lys phase. Note that only the {0,2} *Bragg* peak of the *rac*-DPPE phase was observed in b), the other overlapping with the strong {1,1} and {1, − 1} peaks of *rac*-C_{18}-TE-Lys.

Diastereoisomeric mixtures of oligopeptides of length n labeled (h,d) (where $n = h + d$, h = number of (R)-, and d = number of (S)-repeating units) were obtained, as determined by MALDI-TOF-MS. The experimental relative abundances of the various oligopeptides (defined as the ratio between the amount of a given diastereoisomer and the total amount of all the diastereoisomers of the same length; see *Experimental*) obtained from racemic and (R)/(S) 6:4 monomers, polymerized in the presence of I_2/KI and Ag^+, are shown in *Figs. 2* and *3* relative to those calculated for a theoretical random polycondensation. A random distribution has been experimentally observed

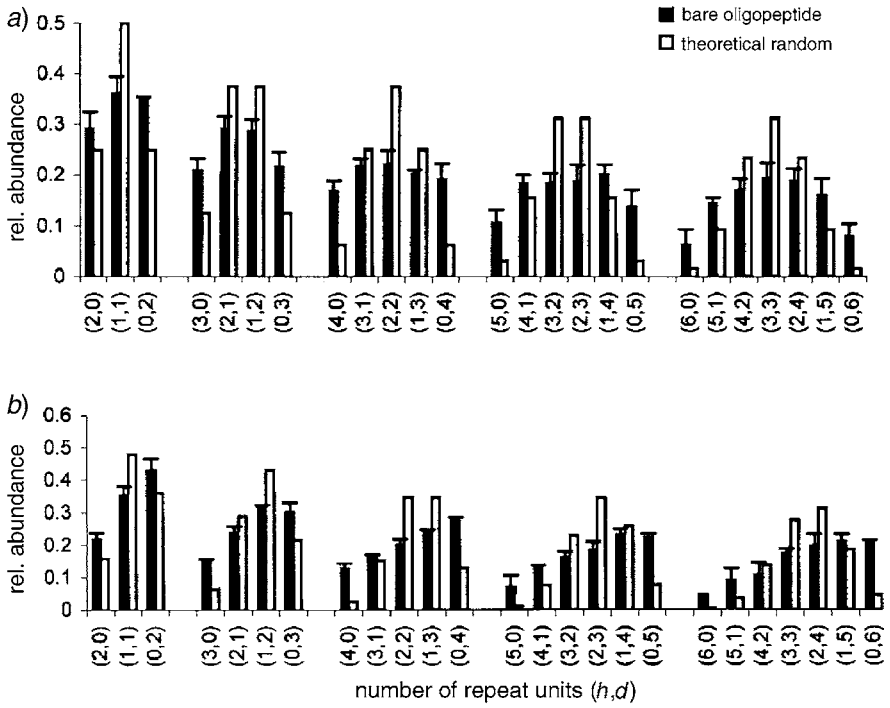

Fig. 2. *MALDI-TOF-MS Analysis of oligopeptides obtained at the air/water interface from equimolar mixtures of* rac-*DPG with* a) *racemic and* b) *nonracemic* ((*R*)/(*S*) 6:4) *C_{18}-TE-Lys, as initiated by I_2/KI*. The histograms show the relative abundance of each oligopeptide (solid bars) relative to those calculated for a binomial distribution in a random process (empty bars). Note that the (*R*)-monomer contained a perdeuterated hydrocarbon chain ($C_{17}D_{35}$).

for γ-stearyl glutamic thioacid, which self-assembles as a two-dimensional solid solution of the two enantiomers [17][18]. The enhancement factors (EF), defined for oligopeptides of various length as the experimental relative abundance of homochiral oligopeptides normalized to the corresponding theoretical values in a random process, are given in *Table 1*. One can see that the dipeptides obtained with both catalysts exhibit an almost random distribution, whereas, for the tri- to hexapeptides, homochiral sequences are overrepresented in all the experiments. This result is similar to that obtained in the absence of *rac*-DPG, which can be rationalized in terms of the packing arrangement of the *rac*-C_{18}-TE-Lys crystallites [17] and a preferred reaction pathway between homochiral monomer [25] molecules along the *a*-axis (*Fig. 4,a*). The composition of the various diastereoisomeric oligopeptides obtained from *nonracemic* ((*R*)/(*S*) 6:4) ratios of C_{18}-TE-Lys mixed with *rac*-DPG (*Figs. 2,b* and *3,b*) shows that, in the presence of *rac*-DPG, the relative abundance of the homochiral peptides with $n = 3-6$ is higher compared to the theoretical random process, which indicates that the (*R*)-monomer, present in excess, was probably separated and reacted to yield homochiral oligopeptides. Similar results were obtained for (*R*)/(*S*) 7:3 ratios of C_{18}-TE-Lys (not shown). The enhancement factors (*Table 1*) obtained in all the

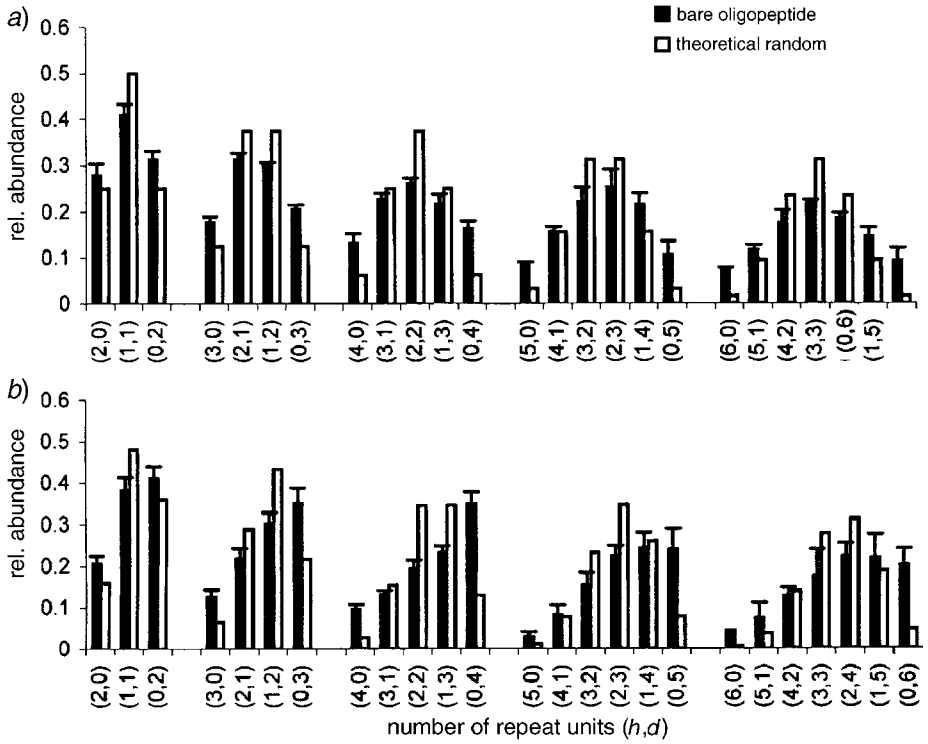

Fig. 3. *MALDI-TOF-MS Analysis of the oligopeptides obtained at the air/water interface from equimolar mixtures of* rac-*DPG with* a) *racemic and* b) *nonracemic* ((*R*)/(*S*) 6:4) *C_{18}-TE-Lys, as initiated by Ag^+*. The histograms show the relative abundance of each experimentally obtained oligopeptide (solid bars) compared to the values calculated for a binomial distribution in a random process (empty bars).

Table 1. *Enhancement Factors* (EF)[a]) *for Homochiral Oligopeptides Obtained in the Polycondensation of Equimolar Mixtures of* rac-*DPG with Racemic* ((*R*)/(*S*) 1:1) *or Nonracemic* ((*R*)/(*S*) 6:4) *C_{18}-TE-Lys.* Two different catalytic systems have been investigated.

No. of Peptide residues	EF for I_2/KI catalysis		EF for Ag^+ catalysis	
	Racemic monomer	Nonracemic monomer	Racemic monomer	Nonracemic monomer
2	1.3	1.2	1.2	1.2
3	1.7	1.6	1.5	1.7
4	2.9	2.6	2.4	2.9
5	3.9	3.3	3.0	3.0
6	4.6	5.0	5.3	4.8

[a]) EF = exper. rel. abundance of homochiral oligopeptides $[(h,0)+(0,d)]_{exp}$ divided by calc. rel. abundance in a random process $[(h,0)+(0,d)]_{cal}$. EF >1 means that a homochiral oligopeptide is overrepresented.

experiments increased with increasing chain length of the oligopeptides, *i.e.*, by 1.5–1.7 for $n=3$; 2.4–2.9 for $n=4$; 3.0–3.9 for $n=5$; and 4.6–5.3 for $n=6$. This is consistent with the formation of tri- to hexapeptides *via* lattice-controlled polycondensation

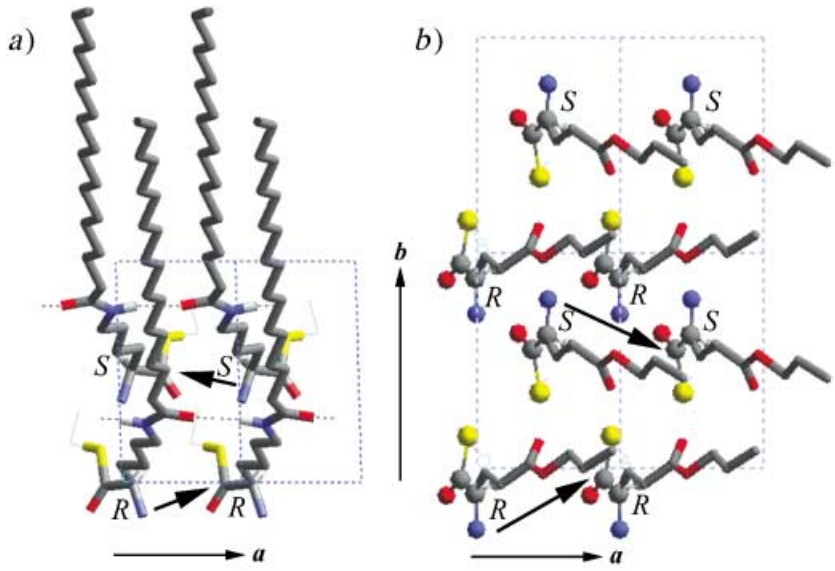

Fig. 4. *Two-dimensional packing arrangements of the racemic crystallites of* a) *C_{18}-TE-Lys and* b) *C_{18}-Te-Glu viewed perpendicular to the water surface.* Note that the reaction pathway is shown with arrows. For clarity, only part of the hydrocarbon chains are shown in b), and the Et group of the thioester is omitted. O-atoms are marked in red, N-atoms in blue, and S-atoms in yellow.

within the racemic crystallites. The results obtained with the two different catalysts were very similar.

b) *DPPE Environment*. The GIXD patterns recorded for 1:1 and 1:2 mixtures of *rac*-DPPE with *rac*-C_{18}-TE-Lys, spread on H_2O, also show a phase separation (*Fig. 1,b*). One phase corresponds to the diffraction pattern of the self-assembled *rac*-C_{18}-TE-Lys crystallites and is very similar to that measured in the absence of DPPE (*Fig. 1,c*) [17]. The second phase arises from the *rac*-DPPE crystallites (*Fig. 1,f*) and displays only the {0,2} *Bragg* peak when compared to the GIXD pattern of the pure phospholipid, the $\{1,1\}+\{1,-1\}$ peak presumably overlapping with the $\{1,-1\}$ peak of the *rac*-C_{18}-TE-Lys crystallites. The *CL*s of the C_{18}-TE-Lys crystallites were affected by the presence of DPPE, being reduced by a factor of two, from 650 and 360 to 320 and 190 Å along the {1,1} and $\{1,-1\}$ directions, respectively. The *CL* in the {0,2} direction of the *rac*-DPPE crystallites was 460 Å.

The GIXD pattern of (*R*)/(*S*) 7:3 C_{18}-TE-Lys mixed in an equimolar ratio with *rac*-DPPE is very similar (not shown) to that obtained from *rac*-C_{18}-TE-Lys (*Fig. 1,b*), *i.e.*, the enantiomorphous phase of the dominating (*R*)-enantiomer was not detected [19]. The presence of the latter could, nevertheless, be demonstrated by MS upon analyzing the enantiomeric composition of the oligopeptides obtained from the polycondensation of deuterium-enantiolabeled C_{18}-TE-Lys in the DPPE environment.

The reason for selecting DPPE was that its NH_2 group may react with C_{18}-TE-Lys, yielding oligopeptides covalently-linked to DPPE, which would support the suggestion that the 2D crystallites of the monomer are embedded in the phospholipid film. Indeed,

diastereoisomeric mixtures of oligopeptides and oligopeptides covalently linked with a DPPE molecule (labeled *P*-(*h*,*d*)) were obtained.

The experimentally determined relative abundances of the various oligopeptides obtained from racemic and nonracemic C_{18}-TE-Lys are shown in *Figs. 5* and *6*, and the corresponding enhancement factors are given in *Table 2*. One can see that the dipeptides obtained with both catalysts exhibit an almost random distribution, whereas the tri-, tetra-, and pentapeptides of homochiral sequence are overrepresented in all the experiments. This result is similar to that obtained with DPG and in the absence of the phospholipid.

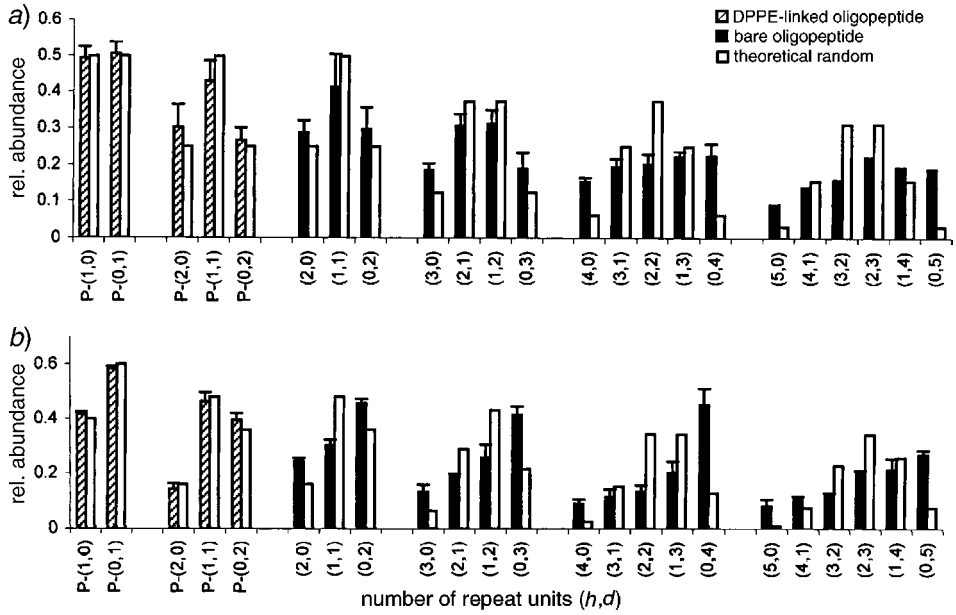

Fig. 5. *MALDI-TOF-MS Analysis of oligopeptides obtained at the air/water interface from equimolar mixtures of* rac-*DPPE with* a) *racemic and* b) *nonracemic* ((*R*)/(*S*) 6 : 4) *C_{18}-TE-Lys, as initiated by I_2/KI*. The histograms show the relative abundance of each experimentally obtained bare oligopeptide (solid bars); DPPE-linked monomer [*P*-(1,0), *P*-(0,1)] and dipeptide [*P*-(*h*,*d*), $h + d = 2$] (hatched bars), and the values calculated for a binomial distribution in a random process (empty bars).

Distinct differences were observed in the formation of the phospholipid-linked oligopeptides [labeled *P*-(*h*,*d*)] as a function of the two catalysts. Only α-amino-acid monomers [*P*-(1,0), *P*-(0,1)] and dipeptides [*P*-(*h*,*d*); $h + d = 2$] were formed with I_2/KI (*Fig. 5*), whereas up to pentapeptides [*P*-(*h*,*d*); $h + d = 5$] were obtained with Ag^+ (*Fig. 6*). This difference can be explained by a complexation of the Ag^+ ion [23] with both the NH_2 group of the phospholipid and the *S*-ethyl group of C_{18}-TE-Lys at the periphery of the crystalline domains of the latter, thus initiating a polycondensation reaction that propagates into the interior of the crystallites. This proposed pathway is supported by the diastereoisomeric distribution of the longer peptides [*P*-(*h*,*d*); $h + d = 3-5$], which is similar to that of the bare oligopeptides (*h*,*d*) initiated within the

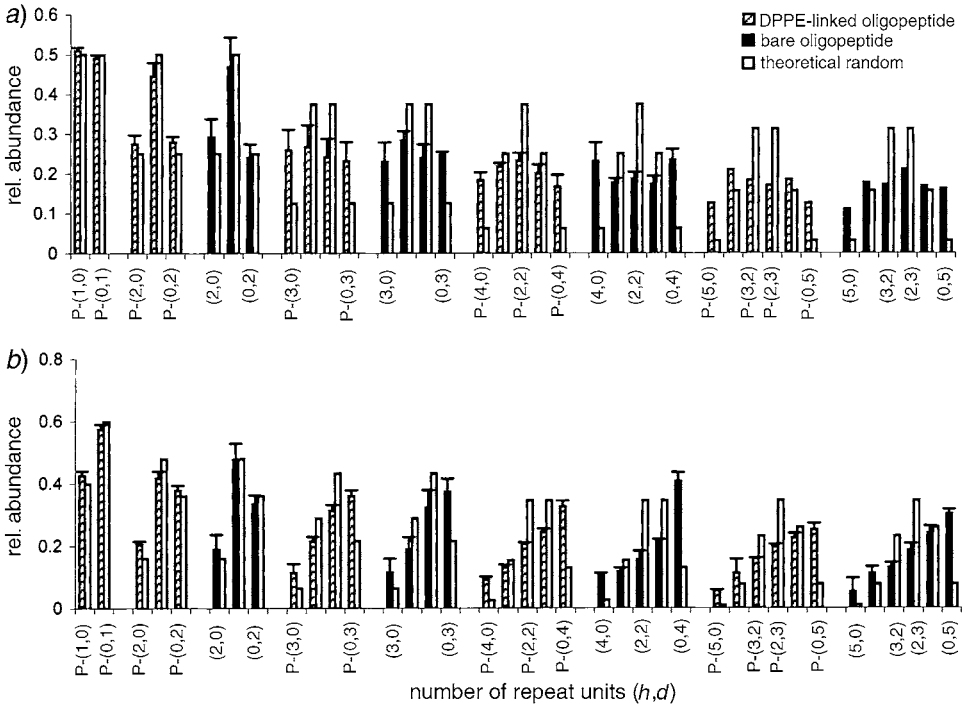

Fig. 6. *MALDI-TOF-MS Analysis of the oligopeptides obtained at the air/water interface from equimolar mixtures of* rac-*DPPE with* a) *racemic and* b) *nonracemic* ((*R*)/(*S*) 6:4) *C_{18}-TE-Lys, as initiated by Ag^+*. The histograms show the relative abundance of each experimentally obtained bare oligopeptide (solid bars), DPPE-linked oligopeptides (hatched bars), and the values calculated for a binomial distribution in a theoretically random process (empty bars).

Table 2. *Enhancement Factors* (EF) *for Homochiral Oligopeptides Obtained in the Polycondensation of Equimolar Mixtures of* rac-*DPPE with Racemic or Nonracemic* ((*R*)/(*S*) 6:4) *C_{18}-TE-Lys*

No. of Peptide residues	EF for I_2/KI catalysis		EF for Ag^+ catalysis	
	Racemic monomer	Nonracemic monomer	Racemic monomer	Nonracemic monomer
2	1.2	1.4	1.1	1.0
3	1.5	2.0	1.9	1.7
4	3.0	3.5	3.7	3.2
5	4.5[a])	4.0	4.3[a])	3.9
2[b])	1.1	1.0	1.1	1.1
3[b])	-	-	2.0	1.7
4[b])	-	-	2.8	2.7
5[b])	-	-	4.0	3.8

[a]) Obtained only in one out of five experiments. [b]) Linked with DPPE.

interior of the crystallites. The phospholipid-linked dipeptides [*P*-(*h*,*d*); $h + d = 2$] exhibit a random distribution and, therefore, are presumably formed in unordered regions of the monolayer.

The GIXD patterns were measured also 2 h after injection of Ag^+ beneath the film (*Fig. 1,e*), showing again phase separation between product phase and DPPE phase.

The composition of the various diastereoisomeric oligopeptides obtained from nonracemic C_{18}-TE-Lys ((*R*)/(*S*) 6:4) mixed with *rac*-DPPE (*Figs. 5,b* and *6,b*) indicates that the relative abundances of the homochiral peptides with $n = 3-5$ is increased compared to the expected random process, which indicates that the (*R*)-monomer, present in excess, was physically separated and reacted to yield homochiral oligopeptides. Similar results were obtained for an (*R*)/(*S*) 7:3 ratio of C_{18}-TE-Lys (not shown).

The enhancement factors given in *Table 2* generally increased with increasing peptide-chain length by factors of 1.5–2.0 for $n = 3$, 3.0–3.7 for $n = 4$, and 3.9–4.5 for $n = 5$, consistent with the formation of tri-, tetra-, and pentapeptides *via* lattice-controlled polycondensation within the racemic crystallites.

Attempts to exert an asymmetric induction in the polycondensation of *rac*-C_{18}-TE-Lys in the presence of enantiomerically pure (*S*)-DPPE were unsuccessful. Both the GIXD patterns and product distributions of mixtures of C_{18}-TE-Lys with (*S*)-DPPE were very similar to those with *rac*-DPPE.

S-*Ethyl Thioester of γ-Stearyl Glutamic Acid*. a) *DPG Environment*. The GIXD pattern of 1:1 mixtures of *rac*-DPG with *rac*-C_{18}-TE-Glu, shown in *Fig. 7,a*, and demonstrates the occurrence of a phase separation. One phase corresponds to the diffraction pattern of the self-assembled *rac*-C_{18}-TE-Glu crystallites and is very similar to that observed in the absence of DPG (*Fig. 7,c*). These crystallites are racemic and contain both enantiomers related by glide symmetry along the *a*-axis (*Fig. 4,b*). The second phase arises from the *rac*-DPG crystalline phase (*Fig. 1,d*). Within the phospholipid environment, the *CL* of crystalline *rac*-C_{18}-TE-Glu was reduced from 400 to 110 Å for the {0,2} *Bragg* peak, but remained unchanged along the {1,1} direction.

The products obtained from the polycondensation of 1:1 mixtures of racemic and nonracemic C_{18}-TE-Glu with *rac*-DPG were analyzed by MALDI-TOF-MS. The products obtained from ten experiments, performed under the same conditions, yielded in some experiments oligopeptides ranging from di- to tetramers, and in others from di- to octamers. These differences may arise from the heterogeneous nature of the reaction. The relative abundance of the homochiral oligopeptides, however, was higher in all experiments compared to the theoretical values expected for a random process. *Fig. 8* shows the distribution of the oligopeptides in three out of five experiments for each mixture. The results are in agreement with a preferential reaction pathway between homochiral molecules along the translational *a*-axis of the monomer crystallites (*Fig. 4,b*). The corresponding enhancement factors are shown in *Table 3* for the trimers to octamers. Only heterochiral dimers were observed, presumably formed at noncrystalline regions of the film. The enhancement factor of the homochiral oligopeptides obtained from the (*R*)/(*S*) 6:4 monomer mixtures appeared to be lower as compared to those obtained from racemic monomer mixtures, reaching a value of 6.0 for the heptamer and 10.8 for the octamer.

b) *DPPE Environment*. The GIXD pattern of 1:1 mixtures of *rac*-DPPE with *rac*-C_{18}-TE-Glu shown in *Fig. 7,b* also indicates a phase separation. The two phases appear similar to those obtained with the pure components (*Figs. 1,f* and *7,c*). Within the phospholipid environment, the *CL* of crystalline *rac*-C_{18}-TE-Glu was reduced from 400

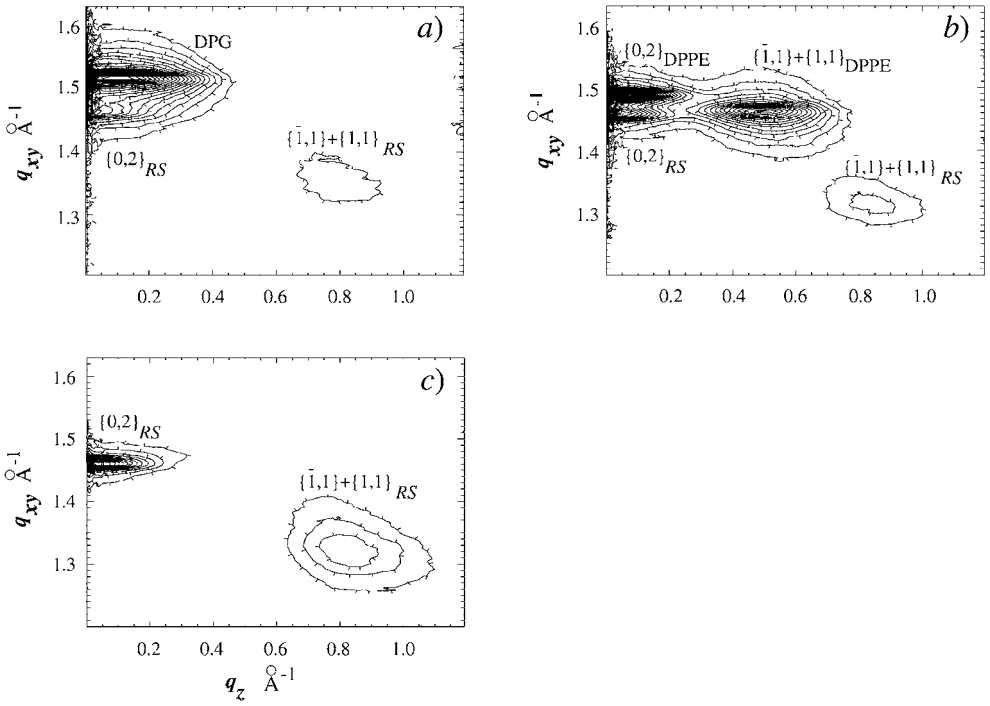

Fig. 7. *GIXD Patterns* (2D contour maps of scattered intensity $I(q_{xy},q_z)$, on H_2O at 4°), *from 2D crystallites self-assembled by spreading $CHCl_3$ solutions of equimolar mixtures of* rac-*C_{18}-TE-Glu with* a) rac-*DPG and* b) rac-*DPPE*; c) *pure rac-C_{18}-TE-Glu*. The *Bragg* peaks are labeled with {*h*,*k*} *Miller* indices, the subscripts '*RS*' refer to the C_{18}-TE-Glu phase.

to 300 Å for the {0,2} *Bragg* peak, but remained unchanged along the {1,1} direction. The *CL* in the {0,2} direction of the *rac*-DPPE crystallites was 340 Å, and 220 Å in the {1,1} direction.

Interestingly, MS analysis showed the formation of homologs only up to pentapeptides covalently linked to one molecule of DPPE (P-(h,d); $h+d=2-5$) for both racemic and nonracemic C_{18}-TE-Glu (*Fig. 9*). The relative abundances of the homochiral oligopeptides is clearly enhanced compared to a random process. The corresponding enhancement factors are given in *Table 3*. The bare oligopeptides were either absent or formed only in trace amounts, which indicates that the polycondensation reaction with Ag^+ was efficiently initiated by DPPE molecules at the periphery of the C_{18}-TE-Glu two dimensional crystallites. As with DPPE/C_{18}-TE-Lys, the diffraction patterns of the *rac*-C_{18}-TE-Glu crystallites with (S)- and *rac*-DPPE were identical, with no asymmetric induction observed in the polycondensation process.

Conclusions. – We have demonstrated by two independent methods that racemic amphiphilic activated α-amino acids self-assemble into two-dimensional crystalline domains within monolayers of phospholipids at the air/water interface. The reactivity within these domains is lattice-controlled, and polycondensation within appropriate

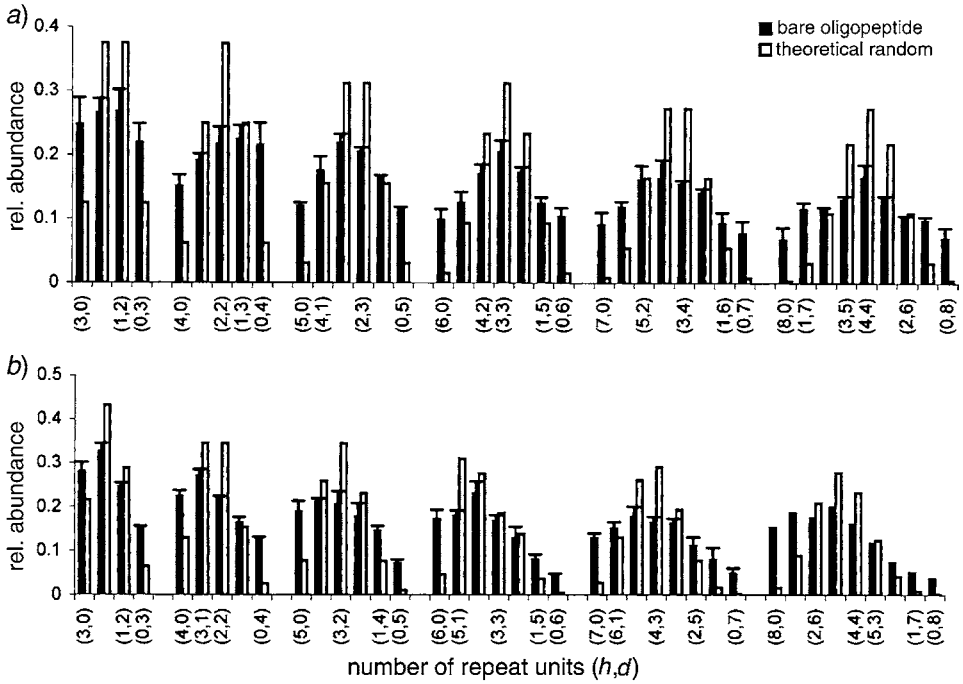

Fig. 8. *MALDI-TOF-MS Analysis of the oligopeptides obtained at the air/water interface from equimolar mixtures of* rac-*DPG with* a) *racemic and* b) *nonracemic* ((*R*)/(*S*) 6 :4) *C_{18}-TE-Glu, as initiated by Ag^+*. The histograms show the relative abundance of each oligopeptide (solid bars) and the values calculated for a binomial distribution in a random process (empty bars). Note that the hydrocarbon chain of the (*S*)-monomer in the (*R*)/(*S*) 6 :4 mixture was perdeuterated ($C_{18}D_{37}$).

racemic architectures gives rise to an enhanced relative abundance of the homochiral (isotactic) oligopeptides. Furthermore, from the MALDI-TOF mass spectra of the condensation products of nonracemic monomers that also show an enhanced formation of homochiral oligopeptides, we deduce that such monomers do not form randomly mixed crystals, but rather undergo phase separation into racemic and enantiomorphous domains. Whereas the two-dimensional crystallites of the phospholipid and of the racemic monomer were observed by X-ray diffraction, the enantiomorphous domains of (*S*)- and *rac*-C_{18}-TE-Glu crystallites displayed very similar GIXD patterns. For the C_{18}-TE-Lys system, a possible line-epitaxial crystallization of (*S*)-C_{18}-TE-Lys alongside the racemic crystallites was proposed [19]. However, phase separation of nonracemic amphiphilic α-amino acids within phospholipids is feasible and was detected by GIXD for an appropriate system (see the following article in this issue [26]).

The formation of oligopeptides covalently linked to a DPPE molecule indicates that the polycondensation reaction, catalyzed by Ag^+ ions, started at the grain-boundaries between DPPE crystallites and those of the racemic or enantiomorphous amino acid monomers. The presence of additional grain boundaries between the racemic and the enantiomorphous monomer domains can also affect the enhancement factors of the homochiral oligopeptides.

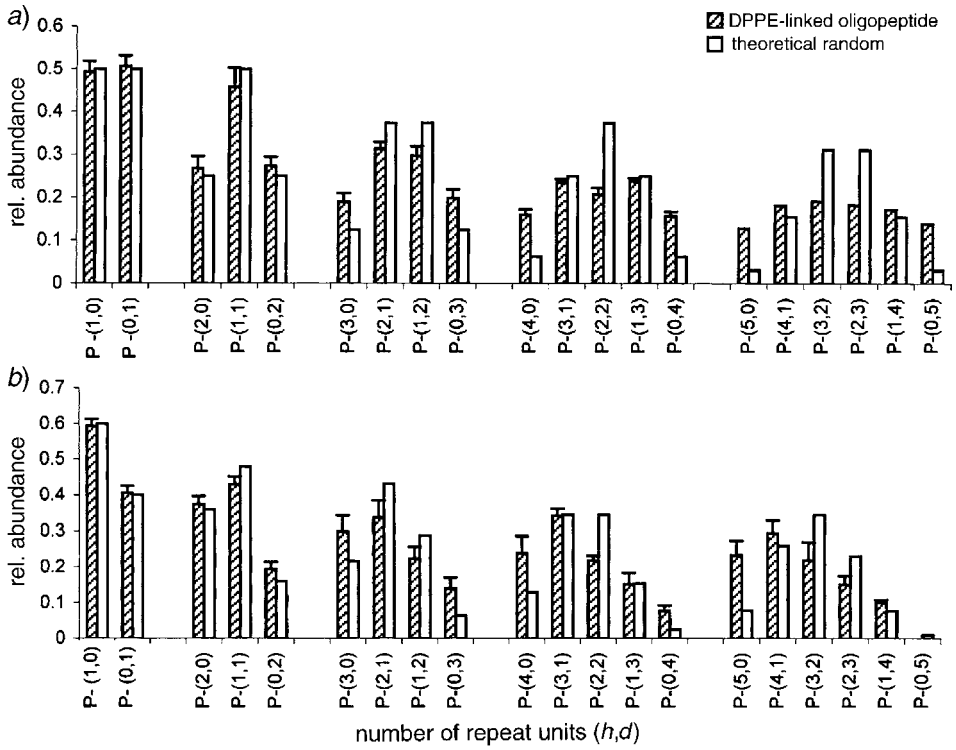

Fig. 9. *MALDI-TOF-MS Analysis of the oligopeptides obtained at the air/water interface from equimolar mixtures of* rac-*DPPE with* a) *racemic and* b) *nonracemic* ((*R*)/(*S*) 6:4) C_{18}-*TE-Glu, as initiated by* Ag^+. The histograms show the relative abundance of each DPPE-linked oligopeptide (hatched bars) and the values calculated for a binomial distribution in a random process (empty bars). Note that the bare oligopeptides were either absent or only formed in trace amounts.

Table 3. *Enhancement Factors* (EF) *for Homochiral Oligopeptides Obtained in the* Ag^+*-Promoted Polycondensation of Equimolar Mixtures of Racemic and Nonracemic* ((*R*)/(*S*) 6:4) C_{18}*-TE-Glu in the Presence of* rac-*DPG and* rac-*DPPE*

No. of Peptide residues	EF with *rac*-DPG		No. of Peptide residues[a])	EF with *rac*-DPPE	
	Racemic monomer	Nonracemic monomer		Racemic monomer	Nonracemic monomer
3	1.9	1.5	2	1.0	1.1
4	2.9	2.2	3	1.6	1.6
5	3.8	3.0	4	2.6	2.0
6	6.5	4.2	5	4.3	2.6
7	10.8	6.0			
8	17.6	10.8[b])			

[a]) Linked with DPPE. [b]) Obtained only in one out of five experiments.

The formation of homochiral oligopeptides from racemates and nonracemic mixtures *via* self-assembly and phase separation *prior* to the polymerization is a

required step in the previously proposed scheme, rationalizing the generation of biopolymers within primitive proto-cells (*Scheme 2*).

Interestingly, the process of enhanced formation of homochiral oligopeptides has a common feature with the nonlinear effects reported in the enantioselective catalysis with non-racemic, chiral auxiliaries described by *Kagan* and co-workers [34]. In both processes, the first step is the self-assembly of the chiral molecules to form small or large diastereoisomeric crystalline architectures of different catalytic or chemical properties. In the nonlinear catalytic amplification reaction, the chiral organometallic dimers or trimers induce the asymmetric autocatalysis, whereas the *meso*-complexes are inert. In the systems described above, the polymerization within the racemic domains yields racemic mixtures of oligopeptides, whereas the monomer in excess, self-assembled as enantiomorphous domains, yields enantiomerically enriched homochiral oligopeptides.

The present results suggest that similar processes might occur also within the bilayer membrane of vesicles that operate as primitive proto-cell systems. Studies along these lines are currently in progress.

Scheme 2. *Possible Scenario for the Generation of Homochiral Oligopeptides under Prebiotic Conditions*

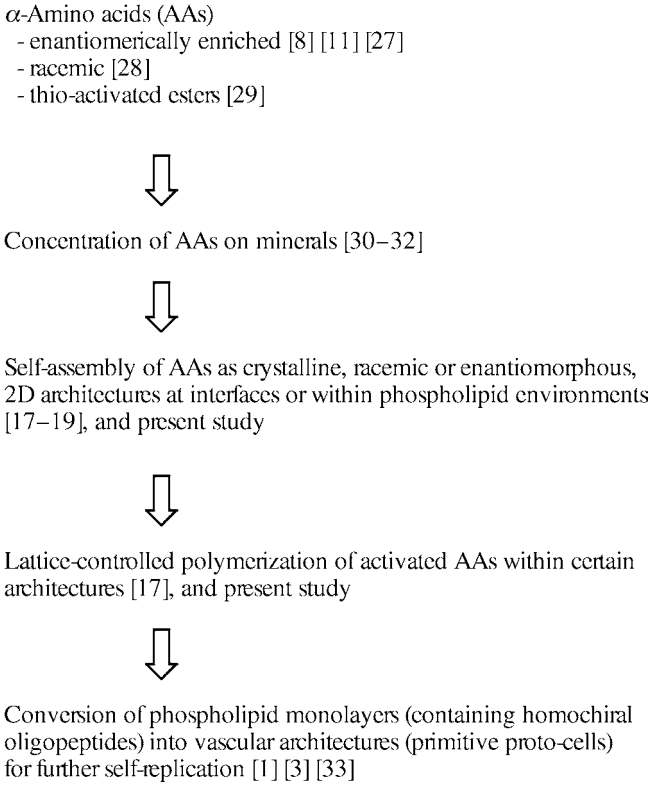

We thank Prof. *L. Leiserowitz* for fruitful discussions and Mrs. *E. Shavit* for the synthesis of the monomers. This work was supported by the *Israel Science Foundation*, the *Petroleum Research Funds of the American Chemical Society*, the *G. M. J. Schmidt Minerva Center*, *The Danish Foundation for Natural Sciences*, and the IHP-Contract HPRI-CT-1999-00040/2001-00140 of the European Commission. We are grateful to HASYLAB at DESY, Hamburg, for beam time at the *BW1* beamline.

REFRENECES

[1] D. W. Deamer, *Microb. Mol. Biol. Rev.* **1997**, *61*, 239.
[2] G. Ourisson, Y. Nakatani, *Tetrahedron* **1999**, *55*, 3183.
[3] P. Walde, R. Wick, M. Fresta, A. Mangone, P. L. Luisi, *J. Am. Chem. Soc.* **1994**, *116*, 11649.
[4] K. Soai, T. Shibata, I. Sato, *Acc. Chem. Res.* **2000**, *33*, 382.
[5] I. Sato, H. Urabe, S. Ishiguro, T. Shibata, K. Soai, *Angew. Chem., Int. Ed.* **2003**, *42*, 315.
[6] I. Weissbuch, L. Addadi, Z. Berkovitch-Yellin, E. Gati, M. Lahav, L. Leiserowitz, *Nature (London)* **1984**, *310*, 161.
[7] D. K. Kondepudi, R. J. Kaufman, N. Singh, *Science* **1990**, *250*, 975.
[8] I. Weissbuch, R. Popovitz-Biro, L. Leiserowitz, M. Lahav, in 'Perspectives in Supramolecular Chemistry', Vol. 1, 'The State of the Art – 100 Years of the Lock-and-Key Principle', Ed. J.-P. Behr, J. Wiley & Sons, New York, 1994, p. 173.
[9] D. K. Kondepudi, K. Asakura, *Acc. Chem. Res.* **2001**, *34*, 946.
[10] W. A. Bonner, E. Rubenstein, G. S. Brown, *Orig. Life Evol. Biosph.* **1999**, *29*, 329.
[11] J. R. Cronin, S. Pizzarello, *Science* **1997**, *275*, 951.
[12] M. Blocher, T. Hitz, P. L. Luisi, *Helv. Chim. Acta* **2001**, *84*, 842.
[13] T. Hitz, M. Blocher, P. Walde, P. L. Luisi, *Macromolecules* **2001**, *34*, 2443.
[14] T. Hitz, M. Blocher, P. Walde, P. L. Luisi, *Macromolecules* **2002**, *34*, 2443.
[15] T. Hitz, P. L. Luisi, *Helv. Chim. Acta* **2002**, *85*, 3975.
[16] T. Hitz, P. L. Luisi, *Helv. Chim. Acta* **2003**, *86*, 1423.
[17] H. Zepik, E. Shavit, M. Tang, T. R. Jensen, K. Kjaer, G. Bolbach, L. Leiserowitz, I. Weissbuch, M. Lahav, *Science* **2002**, *295*, 1266.
[18] I. Weissbuch, G. Bolbach, H. Zepik, E. Shavit, M. Tang, J. Frey, T. R. Jensen, K. Kjaer, L. Leiserowitz, M. Lahav, *J. Am. Chem. Soc.* **2002**, *124*, 9093.
[19] I. Weissbuch, G. Bolbach, H. Zepik, E. Shavit, M. Tang, T. R. Jensen, K. Kjaer, L. Leiserowitz, M. Lahav, *Chem.–Eur. J.* **2003**, *9*, 1782.
[20] C. deDuve, 'Blueprint for a Cell: The Nature and Origin of Life', Neil Patterson, 1991, Chapt. 5.
[21] I. Kuzmenko, H. Rapaport, K. Kjaer, J. Als-Nielsen, I. Weissbuch, M. Lahav, L. Leiserowitz, *Chem. Rev.* **2001**, *101*, 1659.
[22] M. Lahav, F. Laub, E. Gati, L. Leiserowitz, Z. Ludmer, *J. Am. Chem. Soc.* **1976**, *98*, 1620.
[23] L. Zang, J. P. Tam, *J. Am. Chem. Soc.* **1999**, *121*, 3311.
[24] J. C. Sheehan, D. A. Johnson, *J. Am. Chem. Soc.* **1952**, *74*, 4726.
[25] J. G. Nery, G. Bolbach, I. Weissbuch, M. Lahav, *Angew. Chem., Int. Ed.* **2003**, *42*, 2157.
[26] I. Weissbuch, I. Rubinstein, M. J. Weygand, K. Kjaer, L. Leiserowitz, M. Lahav, *Helv. Chim. Acta* **2003**, *86*, 3867.
[27] I. Weissbuch, L. Addadi, M. Lahav, L. Leiserowitz, *J. Am. Chem. Soc.* **1988**, *110*, 561.
[28] S. L. Miller, *Science* **1953**, *117*, 528.
[29] C. Huber, G. Wächtershäser, *Science* **1997**, *276*, 245.
[30] R. Liu, L. E. Orgel, *Origins Life Evol. Biosphere* **1998**, *28*, 245.
[31] J. D. Bernal, 'The Physical Basis of Life', Routledge & Kegen Paul, London, 1951.
[32] G. Cairns-Smith, in 'Frontiers of Life', Eds. J. K. v. T. Thanh, J. C. Mounolou, J. Schneider, C. McKay, Editions Frontières, Gif sur Yvette, 1992, p. 119.
[33] A. Sagathelian, Y. Yokobyashi, K. Soltani, M. R. Ghadiri, *Nature (London)* **2001**, *409*, 797.
[34] C. Girard, H. B. Kagan, *Angew. Chem., Int. Ed.* **1998**, *37*, 2923.

Received September 4, 2003